Atomic structure of the $(2\sqrt{3} \times 2\sqrt{3})R30°$ of silicene on Ag(111) surface

Hanna Enriquez[1,a]**, Abdelkader Kara**[2,b,]**, Andrew J. Mayne** [1,c]**, Gérald Dujardin**[1,d]**, Haik Jamgotchian**[3,e]**, Bernard Aufray**[3,f] **and Hamid Oughaddou**[1,4,g]

[1] Institut des Sciences Moléculaires d'Orsay, ISMO-CNRS, Bâtiment 210, Université Paris-Sud, 91405 Orsay, France

[2] Department of Physics, University of Central Florida, Orlando, Florida, 32816 USA

[3] CINaM-UPR, 7325, CNRS, Campus de Luminy, 13288 Marseille Cedex 09,France

[4] Département de Physique, Bâtiment Neuville II, 5 Mail Gay-Lussac, 95031 Neuville sur Oise, Cergy-Pontoise Cedex, France

E-mail: [a]hanna.enriquez@u-psud.fr, [b]Abdelkader.Kara@ucf.edu, [c]andrew.mayne@u-psud.fr,[d]gerald.dujardin@u-psud.fr, [e]haik@cinam.univ-mrs.fr, [f]aufray@cinam.univ-mrs.fr, [g]hamid.oughaddou@u-cergy.fr,

Abstract. The deposition of one monolayer of silicon on a Ag(111) substrate induces the formation of silicene structures exhibiting different ordered phases, including a $(2\sqrt{3} \times 2\sqrt{3})R30°$, a (4×4) and a $(\sqrt{13} \times \sqrt{13})R13.9°$ superstructures. In this paper we focus on the $(2\sqrt{3} \times \sqrt{3})R30°$ phase. Using a combination of scanning tunneling microscopy and LEED observations, we show that this phase corresponds to a $11°$ rotation of the silicene sheet relative to the substrate orientation.

1. Introduction

Silicene is considered to be a promising novel material for nano-electronics as it will naturally benefits from the vast Si-based Research and Development knowledge (e.g. band gap opening, doping, making electrical contacts, etc)[1, 2]. It has been shown that it has an intrinsic stability and presents electronic properties almost identical to those of graphene [3, 4]. According to theoretical calculations, silicene presents a slight buckling of 0.44 Å between the two inequivalent sublattices, and an in-plane lattice parameter of 3.83 Å [3, 4]. On the other hand, the synthesis of freestanding silicene sheets has progressed only to the stage of silicon nanotubes [5] and multilayer silicene using chemical methods [6]. Thus, growing silicene on solid substrates in particular silver, gold and iridium remains the primary method [7, 8, 9, 10, 11].

Experimentally, the synthesis of silicene has been achieved on the Ag(110) surface where parallel silicene nano-ribbons (NRs) exactly 16 Å wide were obtained [8]. These nanoribbons are potentially very interesting because they have a perfectly well defined edge structure and show 1D dispersion [8] with particular quantum interference effects similar to graphene [12]. To achieve similar results, other 1D structures such as graphene nanoribbons must be synthesized chemically [13], Bi nanolines on Si(001) require a higher formation temperature ($600°C$) [14], and Si nanowires on SiC did not show any 1D conductivity [15].

Now on the Ag(111) surface, a continuous two dimensional (2D) sheet of silicene can be grown. The first experimental study [9] observed the honeycomb silicene structure with a well-defined $(2\sqrt{3} \times 2\sqrt{3})R30°$ superstructure. Soon after this breakthrough, several groups reported the successful growth of silicene on Ag(111) in the $(2\sqrt{3} \times 2\sqrt{3})R30°$ phase, as well as other ordered phases with (4×4) and $(\sqrt{13} \times \sqrt{13})R13.9°$ superstructures [16, 17, 18]. These ordered phases have been interpreted as corresponding to different orientations of the silicene sheet relative to the Ag(111) surface [18, 19].

The $(2\sqrt{3} \times 2\sqrt{3})R30°$ structure was obtained upon deposition of one monolayer of silicon on a Ag(111) substrate kept at a temperature of about $230°C$ [9]. A long-range ordered structure was observed as in both LEED and STM. The STM images show a honeycomb arrangement at the atomic scale, which was interpreted as a local atomic-resolution of a silicene sheet. However, these results were questioned recently due to the small Si-Si first neighbor interatomic distances of 1.9 Å deduced from STM topography [20]. The claim that the STM images do not correspond to a silicene layer but to a bare Ag(111) surface relies on the postulate that the "honeycomb" structure observed is due to a contrast inversion, in other words to a graphically inverted image or to a tip effect [20].

In this paper we present conclusions from a very careful analysis of the STM images on wich accurate drift corrections have been performed. We have determined that the "honeycomb structure" is actually rotated by about 11° with respect to the orientation of the lattice of the bare substrate. In a two-dimensional model of a silicene sheet deposited on a (111) silver layer, we find that this rotation angle of 11° leads to a $(2\sqrt{3} \times 2\sqrt{3})R30°$ superstructure of the substrate, in agreement with the LEED pattern.

2. Experiments

The experiments were performed under ultra-high vacuum (UHV) using the standard tools for surface preparation and characterization: an ion gun for surface cleaning, a low energy electron diffractometer (LEED) for structural characterization, a STM for surface characterization at the atomic scale working at room temperature (RT), and an Auger electron spectrometer (AES) for chemical surface analysis and calibration of the silicon coverage. The Ag(111) sample was cleaned by several cycles of sputtering ($600eV\,Ar^{+}$ ions, $P = 5 \cdot 10^{-5}mbar$) and annealing at $450°C$ until a sharp p(1x1) LEED pattern was obtained. Silicon was evaporated by direct current heating of a piece of Si wafer, and the one monolayer coverage was calibrated using AES. During silicon deposition, the Ag(111) surface was held at a temperature of $(200 - 230)°C$, the temperature being controlled by a thermocouple located close to the sample.

3. Results and discussion

Figure 1 shows the $(2\sqrt{3} \times 2\sqrt{3})R30°$ superstructure observed by LEED after the deposition of one monolayer of silicon on the Ag(111) substrate kept at the above mentioned temperature $(200 - 230°C)$. The unit cell and the spots of the (1x1) are highlighted in figure 1. It is clear from the LEED that a $(2\sqrt{3} \times 2\sqrt{3})R30°$ superstructure has been formed upon deposition of a one monolayer of silicon.

After taking the LEED measurements, the sample was transferred in vacuum for STM measurements. It is important to stress that one needs to perform measurements under the same conditions as the LEED. Because silicene presents many phases, this important step is crucial for assigning the electronic properties to a given phase. Figures 2 (a) and (b) show the STM images obtained respectively on the bare Ag(111) substrate and after the deposition of one silicon ML, that gave the LEED pattern in figure 1. Given there is no rotation of the sample before and after, it is clear that the silicene sheet is rotated by 11° with respect to the bare Ag(111) surface as the pairs of red, green and blue lines show. The STM images were recorded at high current (3 nA) and low bias voltage (-10 mV). The atomic resolved STM images reveal a
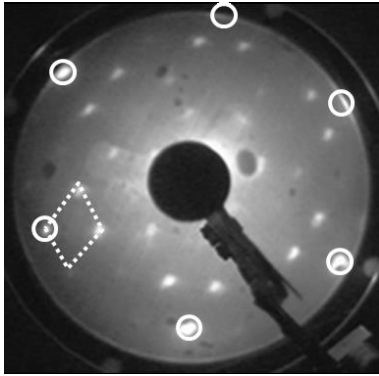
Figure 1. $(2\sqrt{3} \times 2\sqrt{3})R30°$ LEED pattern corresponding to the deposition of 1 silicon monolayer. The unit cell (dotted diamond) and the the spots (small circles) of the (1x1) are highlighted.
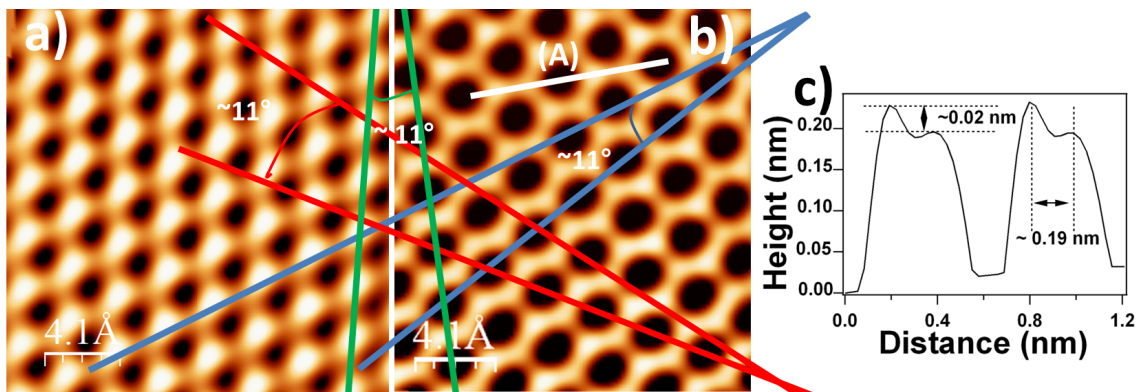
Figure 2. $(2\sqrt{3} \times 2\sqrt{3})R30°$ LEED pattern corresponding to deposition of 1 silicon monolayer. a) A filled-state atomically resolved STM image of the clean Ag(111) surface. b) A filled-state atomically resolved STM image of the same sample after deposition of one silicon monolayer $(U_t = -10mV, I_t = 3nA)$. The pairs of red, blue and green lines show the rotation of the silicene sheet with respect to the clean Ag(111) c) Line-profile joining neighboring Si atoms along the direction (A) indicated in (b).

highly ordered honeycomb lattice silicon structure (Figure 2(b)), while the line profile along line (A) shows a corrugation of 2 Å (from peak to peak) and a height difference between neighboring Si atoms (buckling) of 0.2 Å (Figure 2(c)).

Based on the STM images of the bare Ag(111) (Figure 2(a)), the silicene sheet (Figure 2(b)) and the LEED pattern (Figure 1), we propose the two-dimensional model shown in Figure 3. In this model, a $(\sqrt{7} \times \sqrt{7})R19.1°$ supercell of the silicene sheet coincides with a $(2\sqrt{3} \times 2\sqrt{3})R30°$ supercell of the silver layer.

A 19.1° rotation of the basal chains of the honeycomb silicene sheet gives an effective angle of $(30-19.1)° = 10.9°$ with respect to the axes of the Ag(111, which matches very well our data (Figure 2).

On the basis of the above observations, we can definitely rule out the conclusions of Le Lay et al. claiming that our STM image corresponds to the bare silver surface based on a graphical inversion of the image or due to a tip effect [20]. Indeed, in the case of an inversion of contrast, the angle between the observed honeycomb structure and that of the bare Ag(111) would be 0° as shown in Figure 4. Moreover, the model proposed here and in our previous study [9] is supported by two other recent studies [17, 18].

As we have shown, our careful analysis of the alignment of the observed honeycombs against
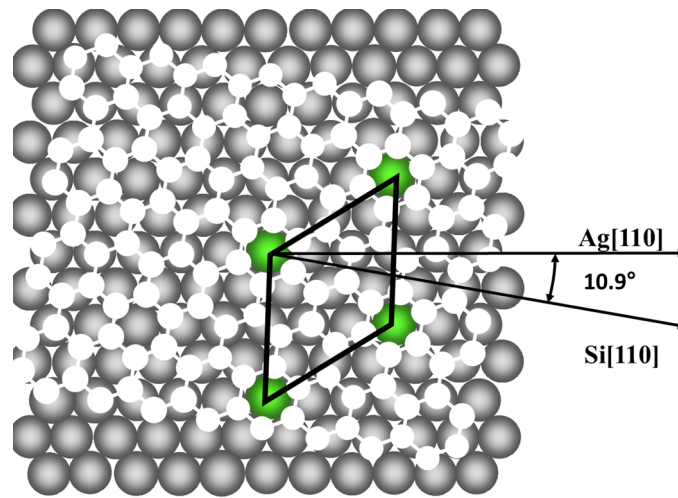
Figure 3. A ball model of silicene on Ag(111) derived from both STM images (Fig 2(a),(b)) and from the observed $(2\sqrt{3} \times 2\sqrt{3})R30°$ LEED pattern shown in Fig 1(a). Silicon and silver atoms are colored in white and grey respectively. Silver atoms showing the $(2\sqrt{3} \times 2\sqrt{3})R30°$ superstructure are colored in green.
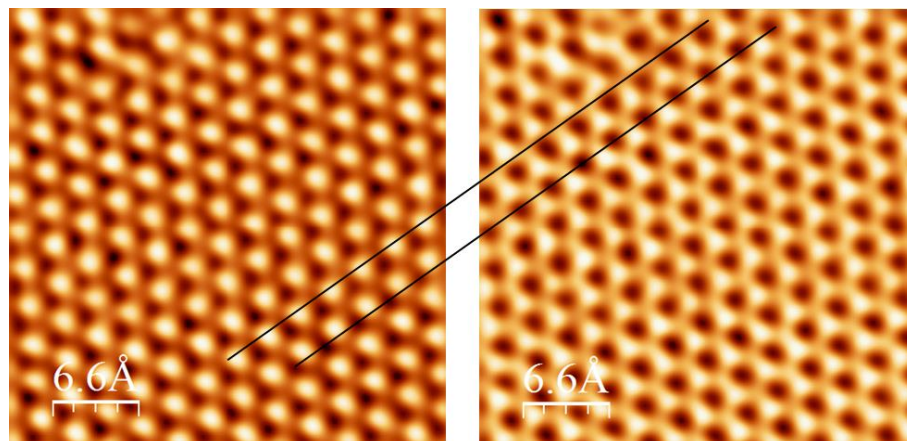
Figure 4. (a) STM image recorded on a clean bare Ag(111)-1x1. (b) graphically inverted image of (a). The axis of the honeycomb-like arrangement resulting from the inversion of the contrast is aligned with the high symmetry axis of figure (a) as highlighted by the parallel dark lines.

the high symmetry direction of the substrate clearly shows an 11° rotation (Figure 2), in agreement with the proposed model (Figure 3). This is irrefutable evidence that STM image in Fig. 2(a) corresponds to a silicene sheet on Ag(111).

Now we will discuss the interatomic distances. The line profile (fig 2c) shows a lateral Si-Si neighbor distance of (1.9 ± 0.1) Å, and not 1.7 Å as has been sometimes stated [16, 20]. This distance is within the range of the values expected for a silicene sheet on Ag(111) [19]. From an experimental point of view, the distance between two protrusions derived from a STM image is not trivial for two reasons. The first is that a projected distance onto the surface plane is a lower bound for the actual interatomic distance. A strong buckling gives a projected distance that is lower than the actual Si-Si distance. The second is a consequence of the STM measurement;

the surface density of states dominates the STM image over the geometrical contribution. In extreme cases, a maximum in the density of states may not correspond to the position of an atom [21, 22]. However, in a recent experiment combining both STM and non-contact atomic force microscopy (AFM) on a silicene sheet in the (4×4) phase, the results clearly show the coincidence between the protrusions in the STM images and the positions of the silicon atoms [23].

Since the maxima in the STM images correspond to the density of states of the Si atoms at the tip position, we can deduce that the actual atomic buckling is more than the observed buckling of 0.2 Å (fig 2c), as is observed on the clean Si(100) 2x1 surface [24]. As a consequence, the apparent lateral Si-Si distance of (1.9 ± 0.1) Å is shorter than the real Si-Si bond length [9, 18, 19]. DFT calculations confirmed that the silicene sheet corresponding to a $(2\sqrt{3} \times 2\sqrt{3})R30°$ superstructure is strongly buckled, with an out-of-plane buckling of 1Å, silicon interatomic distances varying from 2.28 Å to 2.37 Å (giving a projected lateral distance of 2 Å). Due to this strong buckling only two silicon atoms per supercell were imaged in STM topography with a bias voltage of 1V [17, 18] whereas the whole honeycomb atomic structure is resolved in the present study at a bias of 10 mV. This bias dependent behavior has been observed on the clean Si(100) 2x1 surface [24] and also on graphene [25] and is determined by the coupling of the surface states to the bulk [26].

4. Conclusion
In conclusion, we evidence that the honeycomb structure of the $(2\sqrt{3} \times 2\sqrt{3})R30°$ superstructure obtained upon deposition of Si/Ag(111) is due, neither to the inversion of the contrast of the STM image, nor to the contribution of the second silver layer. The orientation of the silicene superstructure deviates by about 11° from that of the substrate. The silicon interatomic distance deduced from STM images is always a lower bound of the actual distance due to the substantial buckling of the adsorbed silicene, in contrast with the flat graphene. The model proposed is in agreement our data and those of other groups [17, 18].

References
[1] Teo B K and Sun X H 2007 *Chem. Rev.* **107** 1454
[2] Dong L, Bush J, Chirayos V, Solanki R, Jao J, Ono Y, Conley J.F and Ulrich B.D 2005 *Nano Letters* **5** 2112
[3] Lebègue S and Eriksson O 2009 *Phys. Rev.* B **79** 115409
[4] Cahangirov S, Topsakal M, Aktürk E, Sahin H and Ciraci S 2009 *Phys. Rev. Lett.* **102** 236804
[5] De Crescenzi M, Castrucci P, Scarselli M, Diociaiuti M, Chaudhari P.S, Balasubramanian C, Bhave T M and Bhoraskar S V 2005 *Appl. Phys. Lett.* **86** 231901
[6] Tchalala M.R, Ait Ali M, Enriquez H, Kara A, Lachgar A, Yagoubi S, Foy E, Vega E, Bendounan A, Silly M, Sirotti F, Nitshe S, Chaudanson D, Jamgotchian H, Aufray B, Mayne A.J, Dujardin G and Oughaddou H, *J. Phys. Condens. Matter* accepted
[7] Kara A, Enriquez H, Seitsonen A P, Lew Yan Voon L C, Vizzini S, Aufray B, and Oughaddou H 2012 *Surface Science Reports* **67** 1
[8] Aufray B, Kara A, Vizzini S, Oughaddou H, Landri C, Ealet B and Le Lay G 2010 *App. Phys. Lett.* **96** 183102
[9] Lalmi B, Oughaddou H, Enriquez H, Kara A, Vizzini S, Ealet B and Aufray B 2010 *Appl. Phys. Lett.* **97** 223109
[10] Tchalala M R, Enriquez H, Mayne A J, Kara A, RothS, Silly M.G, Bendounan A, Sirroti F, Greber T, Aufray B, Dujardin G, Ait Ali M and Oughaddou H 2013 *Appl. Phys. Lett.* **102** 083107
[11] Meng L, Wang Y, Zhang L, Du S, Wu R, Li L, Zhang Y, Li G, Zhou H, Hofer W.A and Gao HJ 2013 *Nanolett* **13** 685
[12] Yang H, Mayne A.J, Boucherit M, Comtet G, Dujardin G and Kuk Y 2010 *Nano Lett.* **10** 943
[13] Van der Lit J, Boneschanscher M P, Vanmaekelbergh D, Ijas M, Uppstu A, Ervasti M, Harju A, Liljeroth P and Swart I 2013 *Nat. Comm.* **4** 2023
[14] Owen J H G, Miki K, Koh H, Yeom H W and Bowler D.R 2002 *Phys. Rev. Lett.* **88** 226104
[15] Soukiassian P, Semond F, Mayne A and Dujardin G 1997 *Phys. Rev. Lett.* **79** 2498
[16] Lin C, Arafune R, Kawahara K, Tsukahara N, Minamitani E, Kim Y, Takagi N and Kawai M 2012 *App. Phys. Exp.* **5** 045802

[17] Feng B, Ding Z, Meng S, Yao Y, He X, Cheng P, Chen L and Wu K 2012 *Nano Lett.* **12** 3507
[18] Jamgotchian H, Colignon Y, Hamzaoui N, Ealet B, Hoarau J Y, Aufray B and Bibérian J P 2012 *J. Phys. Cond. Mat.* **24** 172001
[19] Enriquez H, Vizzini S, Kara A, Lalmi B and Oughaddou H 2012 *J. Phys.Condens. Matter* **24** 314211
[20] Le Lay G, De Padova P, Resta A, Bruhn T and Vogt P 2012 *J. Phys. D* **45** 392001
[21] Knall J, Pethica J B, Todd J D and Wilson J H 1991 *Phys. Rev. Lett.* **66** 1733
[22] Altibelli A, Joachim C and Sautet P 1996 *Surf. Sci.* **367** 209
[23] Majzik Z, Tchalala M R, Ŝvec M, Hapala P, Enriquez H, Kara A, Mayne A J, Dujardin G, Jelínek P and Oughaddou H 2013 *J. Phys. Condens. Matter* **25** 225301
[24] Hata K, Yasuda S and Shigekawa H 1999 *Phys. Rev. B* **60** 8164
[25] Yang H, Cejas C, Mayne A.J, Dujardin G and Kuk Y 2013 *App. Phys. Lett.* **102** 223104
[26] Dujardin G, Mayne A J and Rose F 2002 *Phys. Rev. Lett.* **89** 036802